With arsenic pentafluoride, however, a stable adduct is formed.

Of interest was whether H_2NTeF_5 might behave as an acid. With nitrogen bases (triethylamine, pyridine) reaction was observed, but no definite products were obtained; reactions with CsF or HgF_2 are similar. However, definite derivatives were made by reaction of $R_3SiNHTeF_5$

$$R_3SiNHTeF_5 + CsF \rightarrow R_3SiF + Cs^+NHTeF_5^-$$

$$2R_3SiNHTeF_5 + HgF_2 \rightarrow 2R_3SiF + H_2NTeF_5 + (1/x)[-HgN(TeF_5)-]_x$$

The structure of the mercury compound calls for a comment. Although it is not definitely proven, because of the nonvolatility and insolubility of this compound, its structure is assumed to be a chain -Hg-N-Hg-N-. In contrast with the tetrahedral environment of nitrogen in the long known polymer[6] $[-HgNH_2^+(Cl^-)-]_x$ we have three-coordinated nitrogen in $[-HgN(TeF_5)-]_x$. This may be due to the so-called p_π-d_π back-donation between nitrogen and tellurium. The loss of basity in H_2NTeF_5 may be caused by the same effect.

Acknowledgment. The author wishes to thank Professor W. Sundermeyer for the support of this work and Professor H. Siebert for Raman spectra and helpful discussions.

Registry No. $Me_3SiNHTeF_5$, 42005-82-3; $(Me_3Si)_2NH$, 999-97-3; TeF_6, 7783-80-4; H_2NTeF_5, 42005-83-4; AsF_5, 7784-36-3; $H_2NTeF_5 \cdot AsF_5$, 42005-84-5; $Cs^+NHTeF_5^-$, 42081-47-0; CsF, 13400-13-0; $[-HgN(TeF_5)-]_x$, 42005-81-2; HgF_2, 7783-39-3.

(6) W. N. Lipscomb, *Acta Crystallogr.*, 4, 266 (1951).

Contribution from the Department of Chemistry, The University of Michigan, Ann Arbor, Michigan 48104

Iron(II) and Iron(III) in the Tetrahedral Sulfide Environment of a Gallium Sulfide Host Crystal

JAMES V. PIVNICHNY and HANS H. BRINTZINGER*

Received September 7, 1972

Iron is incorporated into crystals of Ga_2S_3 by chemical transport with hydrogen chloride. Two product phases are formed, and these are separated by careful control of the temperature profile in the crystallization zone. The material deposited at higher temperatures generally contains 5-10% iron by weight and has the γ-Ga_2S_3 structure. The material deposited at lower temperatures has the α-Ga_2S_3 structure and contains 0.1-0.5% iron. In both products the iron content varies with the temperature at which the material is deposited. The iron centers are characterized by means of Mossbauer, epr, and visible and near-infrared reflectance spectra. Most of the iron is in a high-spin iron(II) state and occupies distorted tetrahedral sites in the crystal lattice. The remainder of the iron is in a high-spin iron(III) state and exhibits, in the low-iron material, a rhombic epr signal with apparent g values in the region of 4.3. The visible spectrum of this Fe^{3+} arises from charge-transfer transitions and is consistent with a distorted tetrahedral field. Low-temperature magnetic susceptibility measurements indicate that there is no significant interaction between pairs of adjacent Fe^{2+} centers in the sulfide crystal.

Introduction

In the study of the coordination chemistry of iron, relatively little attention has been directed toward the properties of its ions in a tetrahedral sulfide environment. A tetrahedral coordination geometry has been inferred from spectral data[1-3] and recently established by an X-ray diffraction study[4] for certain iron-sulfur enzymes. The only magnetically and optically dilute, inorganic tetrahedral iron-sulfide system satisfactorily understood to date is that of iron-substituted zinc sulfide.[5-9] In view of the possibility that iron sites of this kind might be intimately involved in such phenomena as the biocatalysis of oxidation-reduction reactions[10] or the electrooptical properties of crystalline sulfide compounds,[11] it appears worthwhile to delineate, in a somewhat more extended scope, the peculiarities of tetrahedral iron-sulfide coordination. In particular, it is of interest to examine the effects of distortions from exact tetrahedral symmetry on the ligand field parameters of iron, the preference of iron for a given oxidation state in this ligand field environment, and the possible existence of metal-metal interaction between iron centers bridged by sulfide ligands. A strong iron-iron interaction, in the form of antiferromagnetic coupling, has been observed in the iron-sulfur enzyme spinach ferredoxin,[12] and its effects are apparent in the characteristic oxidation-reduction properties of this enzyme.

In this study iron ions were incorporated into a host crystal of gallium(III) sulfide since its cation sites, unlike the sites in zinc sulfide, are significantly distorted from tetrahedral symmetry. As with ZnS, the various crystal modifications of gallium(III) sulfide[13] consist of closest packed arrangements

(1) W. A. Eaton, G. Palmer, J. A. Fee, T. Kimura, and W. Lovenberg *Proc. Nat. Acad. Sci. U. S.*, 68, 3015 (1971).
(2) W. R. Dunham, G. Palmer, R. H. Sands, and A. J. Bearden, *Biochim. Biophys. Acta*, 253, 373 (1971).
(3) G. Palmer and H. Brintzinger in "Electron and Coupled Energy Transfer in Biological Systems," Vol. I, Part B, T. E. King and M. Klingenberg, Ed., Marcel Dekker, New York, N. Y., 1972, p 379.
(4) J. R. Herriott, L. C. Sieker, L. H. Jensen, and W. Lovenberg, *J. Mol. Biol.*, 50, 391 (1970).
(5) W. Low and M. Weger, *Phys. Rev.*, 118, 1119 (1960).
(6) R. S. Title, *Phys. Rev.*, 131, 623 (1963).
(7) G. A. Slack, F. S. Ham, and R. M. Chrenko, *Phys. Rev.*, 152, 376 (1966).
(8) J. P. Mahoney, C. C. Lin, W. H. Brumage, and F. Dorman, *J. Chem. Phys.*, 53, 4286 (1970).
(9) A. Gerard, P. Imbert, H. Prange, F. Varret, and M. Wintenberger, *J. Phys. Chem. Solids*, 32, 2091 (1971).
(10) A. San Pietro, Ed., "Non-heme Iron Protein, Role in Energy Conversion," Antioch Press, Yellow Springs, Ohio, 1965.
(11) P. M. Jaffe and E. Banks, *J. Electrochem. Soc.*, 111, 52 (1964).
(12) G. Palmer, W. R. Dunham, J. A. Fee, R. H. Sands, T. Iizuka, and T. Yonetani, *Biochim. Biophys. Acta*, 245, 201 (1971).

of sulfide ions with the cations occupying the tetrahedral interstices. The vacant cation sites in Ga_2S_3 result in a shrinkage of tetrahedra of sulfide ions about these empty sites and, hence, in a distortion of the closest packed anion structure. Gallium(III) sulfide crystals are easily grown by chemical transport reactions,[14,15] and simultaneous transport with small amounts of FeS results in the desired incorporation of iron into Ga_2S_3 host crystals.

Experimental Section

Transport Reactions. Chemical transport reactions were carried out in a horizontal three-zone temperature gradient furnace. The three-zone construction was advantageous in producing uniform temperature gradients and minimizing temperature falloff at the ends of the furnace. In this fashion (see Figure 1), a gradient ranging from 850 to 650°, suitable for the transport of Ga_2S_3, was produced with a long low-temperature part. This region of almost constant temperature represents an ideal crystallization zone and results in a good separation of the different types of product crystals.

Vycor ampoules (cleaned with aqua regia, rinsed, and outgassed at roughly 500° by heating with a hand torch under low pressure of about 10^{-3} Torr) were filled with hydrogen chloride gas (H_2 free) to a pressure of 220–250 Torr at room temperature, resulting in a carrier gas pressure of approximately 1 atm at 650°.

Oxidations. Oxidation reactions were carried out in a sealed ampoule, adding 1 g-atom of sulfur for each gram-atom of iron present in the Ga_2S_3 sample. The ampoule was heated to 700° for a period of 6 hr and subsequently cooled to room temperature. All unreacted sulfur was then sublimed away from the product.

Chemicals and Instruments. Gallium(III) sulfide, 99.99% pure, was obtained from Alfa Inorganics (Beverly, Mass.). Iron(II) sulfide was technical grade obtained from the J. T. Baker Chemical Co. (Phillipsburg, N. J.).

Although the presence of impurities such as oxygen or foreign cations in these materials at a level which could cause interference with conductivity, spin orientation, or other cooperative phenomena cannot be excluded, it is quite unlikely that the spectral properties of iron centers reported here are affected by any impurities. For statistical reasons they could only make a minimal contribution to the immediate environment of the iron centers present and would escape detection by the techniques employed. Furthermore, deliberate addition of small quantities of some of the conceivable trace constituents did not produce measurable changes in the optical properties.

Mossbauer spectra were recorded on a constant-acceleration instrument with a cobalt-57 in copper source maintained at room temperature and a 400-channel analyzer with a scanning rate of 0.02 mm/sec per channel. The instrument was calibrated using iron metal as an external standard, and the reported isomer shifts are relative to this material. Electron paramagnetic resonance spectra were recorded in the X band on a Varian V-4502 spectrometer with 100-kHz modulation. Diffuse reflectance spectra in the visible and near-infrared spectral regions were obtained using a Beckmann DK-2A spectrophotometer with a reflectance sphere attachment, against pure α-Ga_2S_3 as a reference. The temperature dependence of the magnetic susceptibility was measured down to the temperature of liquid nitrogen by the Gouy method. For the liquid helium range of temperatures a vibrating-sample magnetometer with a superconducting coil was employed.[16]

Iron Determinations. Rough estimates of the Fe^{3+} content of low-iron Ga_2S_3 samples were obtained from comparisons of epr signal intensities to those of a standard. Freshly prepared solutions of known concentration of an iron(III) ethylenediaminetetraacetate (EDTA) complex in a 10% water–90% methanol mixture which formed a glass at the cavity temperature (130°K) were used as external standards. The EDTA complex and the Fe^{3+} in Ga_2S_3 exhibit fairly similar signals with apparent g values in the region of 4.3. A piece of polyethylene embedded with phosphorus-doped silicon, which exhibits a $g = 2$ signal, was used as an internal standard to correct for any differences in the sensitivity of the cavity. Signal intensities were determined by a graphical double integration, and iron(III) content was obtained by comparison of the corrected intensities of the sample and the standard. Total iron content was determined colorimetrically *via* the 1,10-phenanthroline complex.[17]

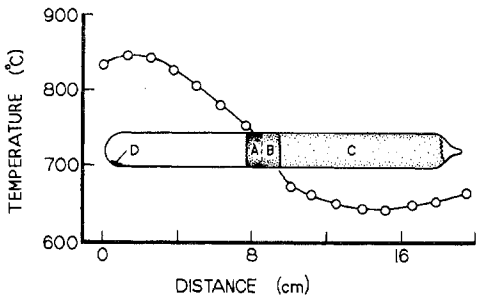

Figure 1. Results of the simultaneous transport of 290 mg of Ga_2S_3 and 9 mg of FeS with HCl gas over a period of 20 hr and the temperature gradient in which it was produced.

Results

Chemical Transport Reactions. Hydrogen chloride gas as a carrier produces cleaner separations of the various product crystals than, for example, iodine. Other sources of iron such as $KFeS_2$, Fe_2O_3, and iron metal were tried, but generally FeS gave the best results. If, for instance, 290 mg of Ga_2S_3 and 9 mg of FeS (2% iron in the starting mixture) were simultaneously transported from 865 to 665° with HCl over a period of 20 hr, three bands of crystalline material were produced (Figure 1). X-Ray powder patterns and chemical iron determinations gave the following properties for these three product materials: A = 29 mg of red-brown crystals having a γ-Ga_2S_3 structure and containing 10.5–11.5% Fe; B = 20 mg of light brown crystals having a γ-Ga_2S_3 structure and containing 5.5–6.5% Fe; C = 241 mg of yellow crystals having the α-Ga_2S_3 structure and containing 0.1–0.3% Fe. The total amount of material recovered was 290 mg, representing 97% of the starting material. The amount of dark residue D was negligible, and no attempt was made to characterize it.

In the γ-Ga_2S_3 structure (products A and B), the sulfide ions are in a cubic closest packing, and the metal vacancies are randomly distributed.[18,19] The α-Ga_2S_3 lattice (material C), a superstructure of β-Ga_2S_3,[19] is approximately hexagonal, but its metal vacancies are arranged in an ordered fashion which, according to Goodyear and Steigmann,[20] results in a monoclinic unit cell. For the further discussion it is important to note that both Ga_2S_3 structures are strictly stoichiometric; *i.e.*, there are no known nonstoichiometric Ga_2S_{3-x} phases. If pure Ga_2S_3 is transported in the absence of FeS, only the α form is produced. The γ form is deposited, at temperatures above the crystallization zone of the α form, only if the product crystals contain an iron admixture in excess of some threshold value which must lie somewhere between 0.7 and 4%. In the transport reaction, the thermodynamics of volatile halide formation is such that the iron content of the product crystals remains at a low value initially, resulting in the exclusive deposition of low-temperature α phase during the first 8–10 hr of the reaction. Only

(13) A. F. Wells, "Structural Inorganic Chemistry," Oxford University Press, London, 1962, p 523.
(14) H. Schafer, "Chemical Transport Reactions," Academic Press, New York, N. Y., 1964.
(15) R. Nitsche, H. U. Bolsterli, and M. Lichtensteiger, *J. Phys. Chem. Solids.*, 21, 199 (1961).
(16) T. H. Moss, D. Petering, and G. Palmer, *J. Biol. Chem.*, 244, 2275 (1969); this magnetometer has a high sensitivity suitable for studies on metal proteins, due to an attainable field of 30 kG.
(17) D. F. Boltz and G. H. Schenk in "Handbook of Analytical Chemistry," L. Meites, Ed., McGraw-Hill, New York, N. Y., 1963, pp 6–26.
(18) H. Hahn and W. Klingler, *Z. Anorg. Chem.*, 259, 135 (1949).
(19) H. Hahn and G. Frank, *Z. Anorg. Allg. Chem.*, 278, 333 (1955).
(20) J. Goodyear and G. A. Steigmann, *Acta Crystallogr.*, 16, 946 (1963).

when the relative iron content of the remaining starting material and, hence, the vapor phase in equilibrium with it have increased by a factor of about 4-5 due to removal of most of the unreacted Ga_2S_3 from the starting material, does deposition of the iron-rich γ form set in at temperatures above those at which α-Ga_2S_3 crystallizes. In the course of the further transport process, γ-Ga_2S_3 of continuously increasing iron content is deposited at increasing temperatures. The occurrence of two distinct zones with different iron contents (A and B) appears to be a consequence of the rather abrupt increase of temperature in this region of the temperature profile (Figure 1; see Table I for the results of several transport reactions).

Spectral Properties of the Iron Centers. The room-temperature Mossbauer spectrum of material A is shown in Figure 2. The spectrum of material B is essentially the same, indicating that these materials differ only in iron content. Values for the isomer shift and quadrupole splitting are IS = 0.64 ± 0.05 mm/sec relative to iron and QS = 3.13 ± 0.05 mm/sec. At 77°K these values are essentially unchanged. The high values of the quadrupole splitting and isomer shift are almost certainly attributes of a high-spin ferrous species. The symmetrical shape of the quadrupole pair indicates that only one kind of iron is present in the material at detectable levels. For the low-iron product a weak spectrum was detected with two peaks that matched those of the high-iron material. Most of the iron in this material is therefore also in the high-spin ferrous state and occupies sites similar to those of the iron in the high-iron material.

The low-iron product exhibits a rhombic epr spectrum with apparent g values in the region of $g' = h\nu/\beta H = 4.3$. This type of signal, which is illustrated in Figure 3, arises from high-spin ferric centers.[21,22] An estimate of the Fe^{3+} content was obtained from the epr signal intensity for six low-iron samples, and the results are given in Table II. In all samples, the amount of Fe^{3+} detected is only a small fraction of the total iron, ranging from 0.05 to 5% of the total iron content. This is in accord with the absence of detectable Fe^{3+} signals in the Mossbauer spectrum of the material.

In order to determine if there is an upper limit to the possible Fe^{3+} content of the low-iron material, we tried to oxidize the Fe^{2+} centers in the host crystal by heating it in a sulfur atmosphere. After the oxidation (see Experimental Section), X-ray powder patterns remained unchanged, but the color of the crystals was noticeably darker than before oxidation. Epr determinations show a definite increase, tenfold or greater, in Fe^{3+} content for some of the samples which had a very low initial Fe^{3+}: total iron ratio (Table II). Even so, the predominant species is still Fe^{2+}, and the Fe^{3+} content does not exceed 5% of the total iron content.

Diffuse reflectance spectra of both the high- and low-iron products in the visible and near-infrared regions are given in Figure 4. The broad peak which begins at 1500 nm, levels off at 2200-2300 nm, and drops slightly thereafter is characteristic of the $^5E \rightarrow {}^5T_2$ transition of high-spin ferrous ion in a tetrahedral environment[23] with a ligand field splitting parameter, Dq, of approximately 440-450 cm^{-1}. Instrumental limitations prevented the recording of the low-frequency parts of the band. A very interesting feature of Figure 4a is the appearance, upon oxidation, of substantial

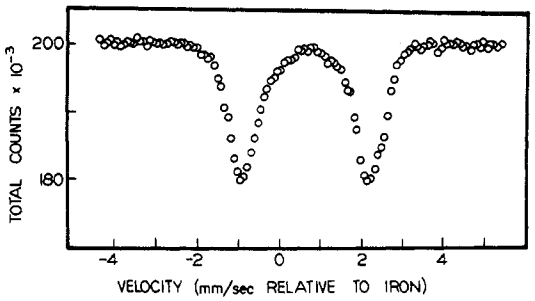

Figure 2. The room-temperature Mossbauer spectrum of a high-iron Ga_2S_3 sample (material A of Figure 1).

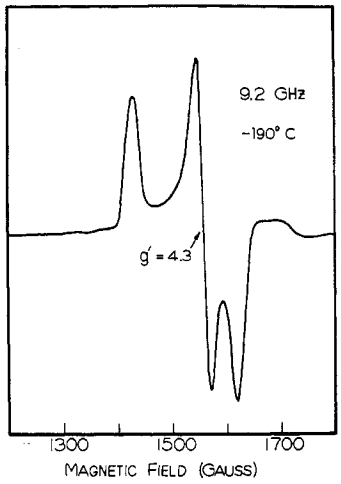

Figure 3. The epr spectrum of a low-iron Ga_2S_3 sample.

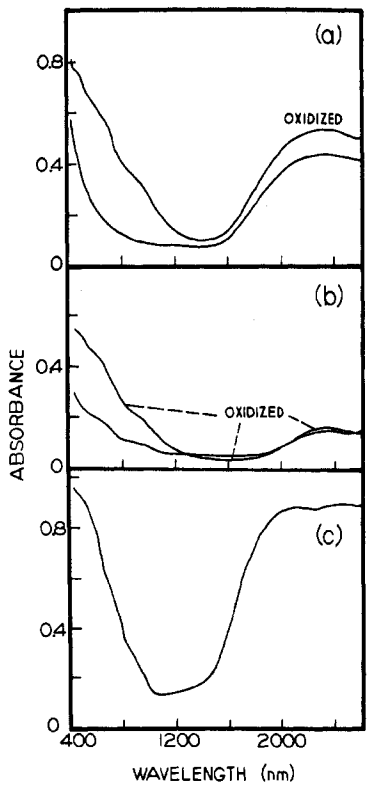

Figure 4. Diffuse reflectance spectra of iron-containing Ga_2S_3 samples: (a) α-Ga_2S_3 containing 0.2% iron and the same material after oxidation in a sulfur atmosphere; (b) α-Ga_2S_3 containing 0.01% iron and its oxidized form; (c) γ-Ga_2S_3 containing 5% iron. In all cases the reference material is α-Ga_2S_3.

(21) W. E. Blumberg in "Magnetic Resonance in Biological Systems," A. Ehrenberg, B. G. Malmstrom, and T. Vanngard, Ed., Pergamon Press, London, 1967, p 119.
(22) R. Aasa, *J. Chem. Phys.*, 52, 3919 (1970).
(23) B. N. Figgis, "Introduction to Ligand Fields," Interscience, New York, N. Y., 1966, p 239.

Table I. Results of Several Transport Reactions

Amt of starting materials, mg		Temp, °C		
Ga_2S_3	FeS	Overall reacn range	Range of γ formn	Range of α formn
389	10	850–680	~760–720	720–680
399	None	850–680	None	720–680
400	10	800–465	~660–545	545–470
410	None	800–465	None	545–470

Table II. Ferric Ion and Total Iron Content of Some Low-Iron Samples

Total iron content[a,b]	Ferric ion content[a,c]	Ferric content[a,c] after oxidn
0.1	5×10^{-3}	
0.2	1×10^{-3}	1×10^{-2}
0.2	3×10^{-3}	
0.3	2×10^{-3}	
0.4	3×10^{-3}	
0.7	3×10^{-4}	8×10^{-3}

[a] Expressed in terms of per cent iron by weight. [b] Determined by the 1,10-phenanthroline method.[18] [c] Determined by a quantitative epr method.

absorptions in the visible region with shoulders at 900, 650, and 450 nm. This can be assigned to the oxidation of a fraction of the Fe^{2+} centers to Fe^{3+} under these conditions. From the strength of its intensity in relation to the low Fe^{3+} concentration, the transitions giving rise to this absorption are most likely charge transfer in nature. Similar observations are obtained with native and oxidized samples containing only 0.01% iron (Figure 4b).

In the spectrum of a sample of the high-iron (5%) material (Figure 4c), the absorption in the near-infrared region is very strong. The strong absorption in the visible region indicates that Fe^{3+} is also present in this material. No epr spectrum was detected for these Fe^{3+} centers. The relatively high iron content of this material probably causes excessive line broadening by spin-spin relaxation. The fraction of iron which is in the 3+ state must be quite small since no Fe^{3+}-type peaks were detected in the Mossbauer spectra of high-iron samples.

Magnetic Susceptibility Measurements. The gram-susceptibility of a high-iron sample containing 7.3% iron followed the Curie-Weiss law with a Weiss constant of −50° between 78 and 294°K. The value of the molar susceptibility of the iron centers, χ_M, at room temperature, corrected for the measured diamagnetism of the Ga_2S_3 host material, was used to calculate an effective magnetic moment according to the expression $\mu_{eff} = 2.83\sqrt{\chi_M T}$. A value of 4.9 BM was obtained which agrees with that expected for high-spin ferrous ions in a tetrahedral site where no first-order spin-orbit coupling exists. Only at temperatures in the vicinity of 4°K did the susceptibility of the same material show significant deviations from the expected behavior for $S = 2$ spin-only centers (Table III).

Discussion

Ferrous Ion Centers. Most of the iron in both the high- and low-iron products exists as high-spin Fe^{2+} ions in the tetrahedral sites of the lattice. This is demonstrated primarily by the position of the d–d band in the near-infrared spectrum. Transitions of similar energy have been detected in the spectra[1,3] of the reduced forms of iron-sulfur proteins with approximate tetrahedral symmetry at the coordination site. Rubredoxin is a particularly good example for comparison purposes because the coordination geometry of its active site with a single isolated iron ion has been determined

Table III. Temperature Dependence of the Gram-Susceptibility ($10^6\chi_g$, cgsu) of a Ga_2S_3 Sample Containing 7.3% Iron

		Temp, °K								
		294	201	170	126	95	78	4.2	2.8	2.2
Obsd	*a*	12.8		19.8	24.4	32.7	34.9			
	b		14.1				28.6	237	295	329
Calcd	*c*	12.9	19.1	22.6	30.7	41.0	50.0	944	1400	1780
	d	11.2	16.4	19.0	24.1	28.9	32.3	12.3	3.4	0.0
	e	11.5	16.9	19.7	25.4	31.3	35.8	199	283	356

[a] Determined on the Gouy balance. [b] Determined in the vibrating-sample magnetometer. [c] Calculated for isolated Fe^{2+} centers with $S = 2$ (spin only). [d] Calculated for coupled Fe^{2+} centers ($S = 2$) with $J = -5$ cm^{-1} [E. A. Earnshaw, B. N. Figgis, and J. Lewis, *J. Chem. Soc. A*, 1656 (1966)]; calculated values include diamagnetism of Ga_2S_3. [e] The mixture of isolated (*ca.* 20%) and coupled (*ca.* 80%) Fe^{2+} centers with $J = -5$ cm^{-1} required by lattice statistics [R. E. Behringer, *J. Chem. Phys.*, 29, 537 (1958)] is in fair agreement with observed values. Higher values of $|J|$ yield values for χ_g which are too low particularly in the region around 100°K; other $|J|$ values or mole fractions of isolated Fe^{2+} centers do not agree with observed χ_g values in the 2–4°K temperature range.

by an X-ray diffraction study.[4] The near-infrared bands of this protein are definitely caused by d–d transitions since their high circular dichroism anisotropy factors, which are greater than 0.01, correspond to magnetic dipole allowed transitions. Assigning the 2200–2300-nm band for iron in Ga_2S_3 to the high-energy component of a slightly split $^5E \rightarrow {}^5T_2$ transition (there may be one or more additional bands beyond the 2600-nm limit of the spectrometer) one obtains a value of somewhat less than 450 cm^{-1} for the ligand field splitting parameter, Dq. McClure[24] has reported that Dq is in the range of 1000 cm^{-1} for Fe^{2+} in the octahedral sites of spinels consisting of closest packed oxide ions. For ferrous ions in a tetrahedral site of the spinel lattice, Dq would be roughly four-ninths of the octahedral value, or in this case, 440 cm^{-1}. A similar, but probably somewhat smaller, ligand field splitting parameter is then indeed expected for a closest packed sulfide structure.

The Mossbauer isomer shift confirms that the ferrous ions are situated in essentially tetrahedral lattice sites. In at least two Mossbauer studies of sulfide minerals,[25,26] it has been reported that isomer shifts are significantly more positive for Fe^{2+} ions in the octahedral sites than in the tetrahedral sites of closest packed sulfide lattice. At room temperature the spinel $FeCr_2S_4$ and stannite, Cu_2FeSnS_4, with ferrous ions in tetrahedral sulfide sites have isomer shifts of 0.60 and 0.57 mm/sec, respectively, relative to iron metal, while the inverse spinel $FeIn_2S_4$ and berthierite, $FeSb_2S_4$, with octahedral ferrous ions exhibit values of 0.88 and 1.08 mm/sec, respectively. The value of 0.64 mm/sec for iron in Ga_2S_3 agrees quite well with the values for tetrahedral ferrous ions. It is also in line with the reported values of iron in cubic and hexagonal zinc sulfide[9] and the reduced form of rubredoxin[27] which are 0.66, 0.69, and 0.59 mm/sec, respectively.

Although the Fe^{2+} sites have thus far been described as tetrahedral, there is in fact a significant distortion of these sites from exact cubic symmetry. Evidence for this is given primarily by the very large quadrupole splitting of 3.15 mm/

(24) D. S. McClure, *J. Phys. Chem. Solids*, 3, 311 (1957).
(25) B. V. Borshagovskii, A. S. Marfunin, A. R. Mkrtchyan, R. A. Stukan, and G. N. Nadzharyan, *Izv. Akad. Nauk SSSR, Ser. Khim.*, 6, 1267 (1968).
(26) N. N. Greenwood and H. J. Whitfield, *J. Chem. Soc. A*, 1697 (1968).
(27) W. D. Phillips, M. Poe, J. F. Weiher, C. C. McDonald, and W. Lovenberg, *Nature (London)*, 227, 574 (1970).

sec even at room temperature. In a strictly tetrahedral ferrous site each of the five d orbitals is occupied by one d electron, and the charge density corresponding to the sixth d electron is shared equally by the $d_{x^2-y^2}$ and d_{x^2} orbitals. This arrangement leads to an isotropic electron distribution; but if a noncubic crystal field component removes the degeneracy of the e level, the charge density is greater in the lower orbital, and the arising field gradient at the nucleus results in a quadrupole splitting. Since the excess charge density in the lowest orbital follows a Boltzmann distribution, the quadrupole splitting will generally increase at lower temperatures. For Fe^{2+} in Ga_2S_3, however, whose room-temperature quadrupole splitting (3.15 mm/sec) is already very high, no significant change was noted when the absorber was cooled to 77°K. This indicates that the energy difference between the two lowest orbitals is much greater than the value of kT at room temperature.

A structural rationale for the high quadrupole splitting for Fe^{2+} in Ga_2S_3 can be obtained (at least in the case of the low-iron α modification) when one notes that the metal sites in α-Ga_2S_3 are actually closer to C_{3v} than to T_d symmetry due to one of the metal-sulfur bonds being approximately 0.1 Å shorter than the other three.[20] For exact C_{3v} symmetry the two d orbitals lowest in energy are again degenerate, but with the axis of quantization taken along the shortened metal-ligand bond, these lowest orbitals are $d_{x^2-y^2}$ and d_{xy}. The charge density of the sixth d electron is then no longer isotropic because it is confined mostly to the xy plane. Thus, a strong electric field gradient is established, and a correspondingly large quadrupole splitting results. Deviations from exact C_{3v} symmetry, which cause a splitting in energy of the $d_{x^2-y^2}$ and d_{xy} orbitals, should do little to increase further the quadrupole splitting since an electron in each of these orbitals gives a similar contribution to the field gradient. The quadrupole splitting should therefore not vary to any great extent with a temperature change. This is consistent with the results obtained for Fe^{2+} in Ga_2S_3. A similar situation is encountered for ferrous ion in rubredoxin[27] whose quadrupole splitting is large and increases only very slightly (3.24 to 3.38 mm/sec) upon going from room temperature to 77°K and does not increase further at 4.2°K.

The distortion which removes the degeneracy of the e set of (approximately) tetrahedral orbitals leads one to expect a similar splitting of the t_2 set, and if the splitting is large, it should be observable in the electronic spectrum as more than a single d-d band. In some of the spectra illustrated in Figure 4, there appears to be a slight increase in absorption at 2600 nm which points to a possible existence of a longer wavelength band beyond the limit of the instrument. If such a band is actually present, a value of lower than 440-450 cm^{-1} for Dq of Fe^{2+} in Ga_2S_3 would be obtained, in reasonable agreement with that of 340 cm^{-1} reported for Fe^{2+} in zinc sulfide.[7] A similar splitting has been observed in the spectrum of ferrous ion in reduced rubredoxin which has the beginning of a band beyond 2500 nm in addition to the maximum recorded at 1600-1700 nm, again in accord with the lower than tetrahedral symmetry of the iron site.

Ferric Ion Centers. The presence of Fe^{3+} in the low-iron Ga_2S_3 lattice is primarily indicated by the rhombic epr signal with $g' = 4.3$. Theoretical treatments of this type of signal have been given by Blumberg[21] and Aasa.[22] Oxidized rubredoxin exhibits a $g' = 4.3$ signal[28] much like that observed for Fe^{3+} in Ga_2S_3. While the structural ubiquity of this type of Fe^{3+} signal precludes any detailed conclusion about the coordination geometries involved, the reflectance spectra in the visible region for iron in Ga_2S_3 do indeed strongly indicate that the ferric site has approximate tetrahedral symmetry.

The absorptions of the Fe^{3+} centers in the visible region can be assigned to charge-transfer rather than d-d transitions on the basis of their intensities. In Figure 4a the intensities of the visible and near-infrared absorptions are comparable even though the Fe^{2+} ions which cause the near-infrared band are present in at least 20 times the concentration of the Fe^{3+} ions which give rise to the visible absorption. Such a large extinction coefficient is highly indicative of charge-transfer transitions.

The charge-transfer spectra of Fe^{3+} in various tetrahedral halide complexes[29] have been studied, and reasonable assignments of the bands have been made, especially in the case of the $FeCl_4^-$ ion. According to Jorgensen's concept of optical electronegativities,[30,31] the energy of the first allowed charge-transfer band for complexes with the same central metal ion should follow the expression $\Delta E_{ct} = (\chi_{opt}[X] - \chi_{opt}[X'])\cdot 30{,}000\ cm^{-1}$, where the χ_{opt} terms denote the optical electronegativities of the ligands X and X'. This expression can also be applied to transitions from lower ligand orbitals, even though these have some metal character and hence energies not entirely independent of the central metal ion. To predict the charge-transfer spectrum of Fe^{3+} in a tetrahedral sulfide site, one can use the known energies of the bands for $FeCl_4^-$ and the Pauling electronegativities[32] of 3.0 for chlorine and 2.5 for sulfur and calculate the expected energies for the sulfide-coordinated iron according to Jorgensen's equation. The allowed charge-transfer transitions for Fe^{3+} in a tetrahedral ligand field are illustrated in Figure 5. Table IV gives the observed energies of these transitions for the $FeCl_4^-$ ion and the predicted energies for the corresponding sulfide complex. The observed maxima and shoulders for the visible spectrum of Fe^{3+} in Ga_2S_3 are included in Table IV, and the agreement with the predicted values is quite good; only the $t_2(L) \rightarrow t_2(M)$ transition predicted to fall at 26,000 cm^{-1} (380 nm) cannot be seen because, if present, it falls under the absorption edge of the Ga_2S_3 conduction band which begins rather abruptly at 400 nm.

A value of $10Dq$ is given by the difference ΔE between the observed energies of the transitions $t_1(L) \rightarrow e(M)$ and $t_1(L) \rightarrow t_2(M)$ since both transitions originate at the same nonbonding ligand orbital. The measured value of $\Delta E = 4500\ cm^{-1}$ for Fe^{3+} in Ga_2S_3 is in the range expected for tetrahedral complexes. The value of $10Dq$ of 4500 cm^{-1} for Fe^{3+} in a tetrahedral site is probably somewhat larger than that estimated above for Fe^{2+} in the same type of site. An increase in the crystal field splitting is to be expected in going from the 2+ to the 3+ oxidation state.

A visible reflectance spectrum of iron substituted into zinc sulfide has been reported[11] in connection with a luminescence study on that material. Three shoulders similar to those for Fe^{3+} in Ga_2S_3 are present, and these are included in Table IV. A total iron concentration of 1 mol % was needed to produce a spectrum with an intensity similar to that produced by 0.2% total iron in Ga_2S_3. Thus, one is led to conclude that the visible spectrum of iron in ZnS is the charge-transfer spec-

(28) J. Peisach, W. E. Blumberg, E. T. Lode, and M. J. Coon, *J. Biol. Chem.*, 246, 5877 (1971).

(29) B. D. Bird and P. Day, *J. Chem. Phys.*, 49, 392 (1968).

(30) C. K. Jorgensen, "Orbitals in Atoms and Molecules, Academic Press, New York, N. Y., 1962, p 94.

(31) C. K. Jorgensen, *Struct. Bonding (Berlin)*, 1, 19 (1966).

(32) L. Pauling, "The Nature of the Chemical Bond," Cornell University Press, Ithaca, N. Y., 1960, p 93.

Table IV. Charge-Transfer Bands for Tetrahedral Ferric Complexes

Transition	Positions of bands, cm^{-1}				
	Chloride[a]	Sulfide (predicted)	Gallium sulfide	Zinc sulfide[b]	Rubredoxin[c]
$t_1(L) \rightarrow e(M)$	27,500	12,500	11,000	12,000	13,500
$t_1(L) \rightarrow t_2(M)$	31,500	16,500	15,500	15,500	17,500
$t_2(L) \rightarrow e(M)$	37,000	22,000	22,000	23,000	20,500
$t_2(L) \rightarrow t_2(M)$	41,200	26,200			26,500

[a] Reference 30. [b] Reference 11. [c] Reference 1; W. Lovenberg and B. E. Sobel, *Proc. Nat. Acad. Sci. U. S.*, 54, 193 (1965).

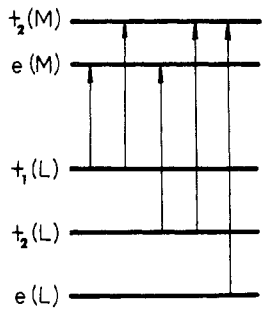

Figure 5. The energy level diagram for a tetrahedral complex including the highest ligand levels (L) and the metal d levels (M). The allowed transitions for a Fe^{3+} complex are indicated.

trum of ferric ion and that the Fe^{3+} accounts for an even smaller fraction of the total iron in the ZnS sulfide, with the remaining iron in the 2+ state. In accord with this, Mossbauer studies of iron in ZnS detected only Fe^{2+}.[9]

While reasonable assignments can be made for the charge-transfer spectra of Fe^{3+} in the tetrahedral metal sulfide crystals, the visible spectrum of oxidized rubredoxin is more complicated. The spectrum of the oxidized protein[33] consists of bands at 280, 350, 380, 490, and 570 nm. In addition, a much weaker band is observed at 750 nm. Its low circular dichroism anisotropy factor of 0.004 indicates that it is magnetic dipole forbidden and therefore not a d-d transition. For this reason it has been assigned to the $t_1(L) \rightarrow t_2(M)$ transition in Table III. A value for the crystal field splitting of 4000 cm^{-1} for Fe^{3+} in rubredoxin can be obtained from the difference of the energies of the 750- and 570-nm bands when these are assigned to the $t_1(L) \rightarrow e(M)$ and $t_1(L) \rightarrow t_2(M)$ transitions, respectively. No other combination of the longer wavelength bands gives such a reasonable value.

If, in fact, the 750-nm (13,500 cm^{-1}) band is the first charge-transfer band for rubredoxin, it appears that the optical electronegativity of mercaptide sulfur in the apoprotein is somewhat higher than that of sulfur in a metal sulfide lattice since the first charge-transfer bands for both Fe^{3+} in Ga_2S_3 and Fe^{3+} in ZnS fall at longer wavelengths (850 and 900 nm). A higher optical electronegativity is to be expected with mercaptide sulfur since it is less polarizable than sulfide ion with some of its electron density being located in a sulfur-carbon single bond.

Strength of Iron-Iron Interactions. In those samples where the iron content of the Ga_2S_3 host material reaches a level of about 10%, the majority of the Fe^{2+} centers present will no longer be isolated but will have iron neighbors in one or more of the adjacent cation sites. An adoption of the statistics developed by Behringer[34] to the Ga_2S_3 structure allows one to calculate that more than 75% of the iron centers will occur in pairs, triples, or other multiples at these iron concentration levels. Any strong antiferromagnetic interaction between these adjacent iron sites must result in a significant deviation of magnetic susceptibilities from the Curie law. Comparison of the magnetic data obtained (Table III) with those predicted[35] for antiferromagnetically coupled pairs of $S = 2$ centers shows, however, that a value of $J = -5$ cm^{-1} is an upper limit for the magnitude of the antiferromagnetic coupling constant for adjacent Fe^{2+} centers. Since a second-order spin-orbit coupling similar to that observed for isolated Fe^{2+} centers in zinc sulfide[8] will most likely also occur for Fe^{2+} in Ga_2S_3 and, hence, contribute to the observed decrease of μ_{eff} at temperatures in the vicinity of 4°K, the true value of the antiferromagnetic coupling constant may very well be even smaller than 5 cm^{-1}.

We consider it an important result of this study that strong interactions between Fe^{2+} centers do not occur ($J \approx -5$ cm^{-1}) when their coordination tetrahedra are bridged by a single sulfide ligand with an Fe-S-Fe angle in the vicinity of 109°.[36] For the iron centers in polynuclear ferredoxins it follows that the strong Fe-Fe coupling observed in these proteins—whatever its detailed electronic mechanism—must be intimately connected with a structure in which each pair of adjacent FeS_4 coordination tetrahedra shares two sulfide ligands of a tetrahedral edge.

The largely similar physical properties of iron centers in a Ga_2S_3 host crystal and in proteins like rubredoxin demonstrate that the solid state can stabilize unusual coordination numbers and geometries of transition metals in a manner surprisingly similar to that occurring in metalloproteins. As for the oxidation-reduction properties of iron centers in the sulfide lattice it appears that the upper limit of Fe^{3+} concentration attainable is a thermodynamic function connected to the Fermi level in the host crystals; this limit is essentially unaffected by factors such as the relative numbers of surface and bulk sites or of isolated and adjacent iron sites. The ease with which iron centers in the interior of the host crystal are oxidized upon exposure of the bulk crystals to a sulfur atmosphere, thus indicating a connection between the electron population in the iron d orbitals with that of the sulfide band structure, is reminiscent of the related problem of electron transfer mechanisms to and from iron sites buried in the interior of redox-active iron-sulfur proteins.[37]

Acknowledgments. We express our appreciation to Dr. Graham Palmer, who helped in obtaining epr spectra, and Dr. B. J. Evans for measuring some of the Mossbauer spectra. We are greatful to Dr. J. W. Mann and the Climax Molybdenum Co. of Michigan for making available the spectrometer used to record the reflectance spectra and Dr. Tom Moss and Mr. Charles Moleski of the IBM Watson Research Laboratories who provided the magnetic measurement at liquid helium temperatures. Discussions with all these colleagues were extremely valuable.

Registry No. Ga_2S_3, 12024-22-5; Fe^{2+}, 15438-31-0; Fe^{3+}, 20074-52-6.

(33) W. Lovenberg and B. E. Sobel, *Proc. Nat. Acad. Sci. U. S.*, 54, 193 (1965).
(34) R. E. Behringer, *J. Chem. Phys.*, 29, 537 (1958).
(35) A. Earnshaw, B. N. Figgis, and J. Lewis, *J. Chem. Soc. A*, 1656 (1966).
(36) That the Fe-O-Fe angle at a bridging oxo ligand is critical for the magnitude of the spin-spin coupling constant is well documented: J. Lewis, F. E. Mabbs, and A. Richards, *J. Chem. Soc. A*, 1014 (1967); H. J. Schugar, G. R. Rossmann, and H. B. Gray, *J. Amer. Chem. Soc.*, 91, 4564 (1969).
(37) A. Mildvan, G. Palmer, and R. W. Estabrook in "Magnetic Resonance in Biological Systems," A. Ehrenberg, *et al.*, Ed., Oxford University Press, London, 1967, p 175.